Neurotherapeutics 22 (2025) e00569

Contents lists available at ScienceDirect

Neurotherapeutics

journal homepage: www.sciencedirect.com/journal/neurotherapeutics

Original Article

Tumor suppressive effect of low-frequency repetitive transcranial magnetic stimulation on glioblastoma progression

Seongmoon Jo [a,b,c,1], Sang Hee Im [a,1], Sung Hoon Kim [d], Dawoon Baek [a,d,e], Jin-Kyoung Shim [f,g], Seok-Gu Kang [f,g], Jong Hee Chang [g], Geneva Rose Notario [a,b], Do-Won Lee [a], Ahreum Baek [a,d,h,*], Sung-Rae Cho [a,b,i,j,k,*]

[a] Department and Research Institute of Rehabilitation Medicine, Yonsei University College of Medicine, Seoul, South Korea
[b] Graduate School of Medical Science, Brain Korea 21 Project, Yonsei University College of Medicine, Seoul, South Korea
[c] Division of Hematology, Department of Medicine, Washington University in St. Louis, St. Louis, MO 63110, USA
[d] Department of Rehabilitation Medicine, Yonsei University Wonju College of Medicine, Wonju, South Korea
[e] Forensic DNA Division, Daegu Institute, National Forensic Service, Chilgok-gun, South Korea
[f] Department of Neurosurgery, Brain Tumor Center, Severance Hospital, Yonsei University College of Medicine, Seoul, South Korea
[g] Brain Tumor Translational Research Laboratory, Severance Biomedical Research Institute, Yonsei University College of Medicine, Seoul, South Korea
[h] Department of Clinical Laboratory Science, Semyung University, Jecheon, South Korea
[i] Graduate Program of Biomedical Engineering, Yonsei University College of Medicine, Seoul, South Korea
[j] Rehabilitation Institute of Neuromuscular Disease, Yonsei University College of Medicine, Seoul, South Korea
[k] Brain Research Institute, Yonsei University College of Medicine, Seoul, South Korea

ARTICLE INFO

Keywords:
Repetitive transcranial magnetic stimulation
Low-frequency
Glioblastoma
Tumor suppression effect

ABSTRACT

Repetitive transcranial magnetic stimulation (rTMS) is used as a non-invasive treatment for various diseases, and its potential application in cancer treatment has been proposed by researchers. However, the precise mechanisms and effects of rTMS on many types of cancer, including glioblastoma (GBM), remain largely unknown. This study aimed to investigate the effects of low-frequency rTMS on *in vitro* and *in vivo* GBM models and to elucidate an underlying biological mechanism of rTMS on GBM. *In vitro* and *in vivo* GBM models were treated with low-frequency rTMS (0.5 Hz, 10 min per day), and the effects of rTMS were assessed using various assays, including CCK-8 assay, sphere formation assay, 3D invasion assay, RT-qPCR, Western blot, immunohistochemistry, TUNEL assay, MRI, and IVIS. The results showed that treatment of GBM models *in vitro* with low-frequency rTMS significantly inhibited cell proliferation. Transcriptome array analysis revealed a substantial downregulation of FLNA and FLNC expression after low-frequency rTMS treatment. Moreover, in an *in vitro* GBM tumor sphere model, low-frequency rTMS suppressed the activation of EGFR and EphA2, inhibited ERK/JNK/p38 and PI3K/AKT/mTOR pathways, and induced apoptosis. Low-frequency rTMS also suppressed the invasion of GBM by downregulating MMP2 and MMP9 expression. Additionally, in an *in vivo* GBM model, low-frequency rTMS suppressed GBM progression by downregulating FLNA and FLNC expression. The results demonstrated that low-frequency rTMS could be a potential treatment for GBM, achieved by downregulating FLNA and FLNC expression. This study sheds light on the potential for rTMS as a therapeutic strategy for glioblastoma as well as other types of cancers.

Abbreviations: MS, Magnetic stimulation; rMS, Repetitive magnetic stimulation; rTMS, Repetitive transcranial magnetic stimulation; TS, Tumor sphere; DMEM, Dulbecco's modified Eagle's medium; FBS, Fetal bovine serum; OD, Optical density; CCK-8 assay, Cell counting kit-8 assay; RNA-seq, RNA Sequencing; GO, Gene ontology; DAVID, Database for annotation, visualization and integrated discovery; FLNA, Filamin A; FLNC, Filamin C; PI3K, Phosphatidylinositol-4,5-bisphosphate 3-kinase; ERK, Extracellular signal-regulated kinase; JNK, c-Jun N-terminal kinase; AKT, AKT Serine/Threonine kinase; mTOR, Mechanistic target of rapamycin; Bax, Bcl-2 associated X, apoptosis regulator; Bcl-2, B-cell lymphoma 2; MMP2, Matrix metalloproteinase-2; MMP9, Matrix metalloproteinase-9; MMPs, Matrix metalloproteases; TUNEL, Terminal dUTP Nick End-Labeling; TMZ, Temozolomide; DEGs, Differentially expressed genes; mT, millitesla.

* Corresponding authors.
E-mail addresses: ahreumbaek@semyung.ac.kr (A. Baek), srcho918@yuhs.ac (S.-R. Cho).
[1] These authors contributed equally to this work.

https://doi.org/10.1016/j.neurot.2025.e00569
Received 6 November 2024; Received in revised form 2 February 2025; Accepted 28 February 2025

Introduction

Repetitive transcranial magnetic stimulation (rTMS) is a non-invasive method for stimulating the brain by generating a pulsed magnetic field through the intact scalp and inducing localized electric currents in the underlying cortical microenvironment [1,2]. Due to its ability to stimulate specific areas of the brain with minimal invasiveness, many researchers have attempted to utilize rTMS to treat numerous neurological disorders [3]. The effects of rTMS vary depending on the specific rTMS protocol employed, which is determined by several factors, such as stimulus frequency, stimulus intensity, and the total number of stimuli [4]. Although most research into the potential clinical uses of rTMS has focused on the treatment of depression, various rTMS protocols have been made available to address many kinds of disorders, each with distinct approaches [5–7]. Accordingly, there are many studies focused on the optimization of rTMS to treat diseases including tic disorder, intractable seizures, schizophrenia, stroke, Parkinson's disease, and Alzheimer's disease [8–13].

Glioblastoma (GBM) is a form of cancer characterized by primary tumor occurring in the central nervous system (CNS), particularly in the brain [14]. The overall prognosis of GBM remains poor, with patients having a low survival rate [15]. The current standard treatment for GBM patients consists of aggressive surgical techniques for complete resection of the tumor mass and adjuvant therapies, such as radiation therapy, chemotherapy, or a combination of these [16]. Despite recent advances, it is still hard to improve the life expectancy of patients with GBM [17]. Therefore, more effective and less toxic treatments must be developed to lessen the burden on patients.

Recent studies have indicated that rTMS is a feasible method for treating cancer patients. As a non-invasive neuroimaging technique, rTMS allows for preoperative mapping of the brain before surgery to plan for the safe resection of brain tumors [18]. In addition, recently emerging evidence suggests that rTMS can be effective in the neurorehabilitation of patients who have undergone brain tumor surgery by improving their motor and language abilities [19]. Moreover, there are some reports suggesting that rTMS may have an effect on tumor progression by suppressing tumoral development while stimulating immune functions [20,21]. It has also been indicated that magnetic field stimulation has the potential to affect glioma cells by preventing cell proliferation and reducing cell viability [22].

In previous studies, low-frequency repetitive magnetic stimulation (rMS) was found to reduce cell proliferation, while high-frequency rMS increased cell proliferation [23–25]. Moreover, research using low-frequency rTMS in neuroblastoma models showed a tumor suppressive effect [26]. In light of the results of these studies, this investigation aims to further investigate the tumor suppressive effect of low-frequency rTMS on both *in vitro* and *in vivo* GBM models with the goal of elaborating on the therapeutic effects and mechanisms of low-frequency rTMS on GBM.

Materials and methods

Cell culture

The U-87 MG (U87MG) cell line (RRID: CVCL_0022) was obtained from the American Type Culture Collection (Manassas, VA, USA). U87MG cells were incubated in a humidified 5 % CO_2 incubator at 37 °C with Dulbecco's modified Eagle's medium (DMEM; Hyclone, Logan, UT, USA) containing 10 % fetal bovine serum (FBS; Serum Source International, Charlotte, NC, USA) and 1 % penicillin/streptomycin (Gibco, Rockville, MD, USA). The medium was replaced at three-day intervals.

U87MG cells were seeded at a density of 1×10^6 cells per 100 mm plate. Trypsin-EDTA was used to dissociate confluent cells.

Tumorsphere culture

Two primary tumor cell lines, TS15-88 and TS21-117, were established from fresh GBM tissue specimens, as approved by the institutional review board of the Yonsei University College of Medicine (4-2021-0001). U87MG TS cell and primary GBM cells were cultured under serum-free, non-adherent conditions to promote tumor sphere formation. This culture method was used to recapitulate key characteristics of actual tumors, maintaining tumor cellular functions essential to GBM progression, akin to those observed in primary cells. Briefly, cells were harvested using Trypsin-EDTA, washed with PBS, and resuspended in a serum-free medium composed of DMEM/F-12 (Mediatech, Manassas, VA, USA) with 1X B27 (Invitrogen, Carlsbad, CA, USA), 20 ng/mL of bFGF, 20 ng/mL of EGF (Sigma-Aldrich, St. Louis, MO, USA), and 1 % penicillin/streptomycin. The cells were plated at a density of 1×10^4 cells/mL per ultra-low attachment 96-well plate. Cells were incubated at 37 °C in a humidified atmosphere with 5 % CO_2. Following the observation of sphere formation in 24 h, treatments and subsequent experiments were performed.

Plasmids and cell transfection

FLNA or FLNC overexpression plasmids (CAT# RC221764, CAT# RC212462) and the negative control (NC) empty pCMV6 vector (CAT# PS100001) were purchased from Origene (Rockwill, MD, USA). Under normal cell culture conditions, U87MG cells were transfected with 1 μg control vector, FLNA, or FLNC using Lipofectamine 3000 (Invitrogen, Carlsbad, CA, USA) according to manufacturer instructions. After 24 h, transfected U87MG cells were cultured in tumor sphere culture conditions to generate transfected U87MG TS, and subsequent experiments were performed.

Repetitive transcranial magnetic stimulation

Before stimulation, cell growth medium was replaced in each experiment. *In vitro* GBM models were stimulated with customized repetitive magnetic stimulation (Bicon-1000Pro, Mcube Technology, Seoul, Korea). Stimulation intensity was set to 18 mT and was delivered as a monophasic pulse with a rise time of 370 μs. The frequency and amplitude of the stimulation were monitored with a probe connected to a digital multimeter and an oscilloscope, as described in previous studies [24–26]. Cells were stimulated for 10 min each day over a 3-day period. The distance between the center of the magnetic coil (70-mm diameter) and the culture dish was approximately 1.0 cm, and the magnetic coil did not generate heat during stimulation, as confirmed with the thermal sensor and cooling system implanted in the customized rMS. The *in vitro* GBM models were divided into two groups: a sham group, in which culture dishes were placed without rMS, and a low-frequency treatment group, which received 0.5 Hz stimulation at an on-off interval of 3 s. After magnetic stimulation, cells were harvested for further experiments (Fig. 1A).

Cell counting Kit-8 (CCK-8 assay)

CCK-8 assays were performed according to the manufacturer's instructions (Dojindo, Kumamoto, Japan). Briefly, *in vitro* GBM models were cultured in 96-well plates. After treatment, 10 μl of the kit reagent was added to each well. Following incubation at 37 °C for 1 h, optical density (OD) was measured at 450 nm using a multifunctional microplate reader (VersaMax, Molecular Devices, San Jose, CA, USA).

Sphere formation assay

For the sphere formation assay, GBM TSs were cultured in 96-well plates as mentioned above.

Following treatment, wells containing successfully formed tumor spheres were designated as sphere-positive and included in the analysis, while wells without tumor sphere formation were excluded from the count. The number of sphere-positive wells in the low-frequency group relative to the sham group was calculated and presented as a percentage. To determine TS morphology and size, GBM TSs were observed with an inverted phase-contrast microscope (I × 71 Inverted Microscope; Olympus, Tokyo, Japan) and imaged with a digital camera (DP70 Digital Microscope Camera; Olympus) [27].

3D invasion assay

To evaluate the migratory capacity of cancer cells, which is a critical hallmark of cancer progression and metastasis, a 3D invasion assay was performed on U87MG, TS15-88 and TS21-117 cells. Each single spheroid was seeded and cultured in individual wells of a 96 well plate containing a mixed matrix composed of Matrigel (BD Biosciences, Bedford, Mass, USA), collagen type I (Corning Incorporated, Corning, NY, USA), and TS complete media. Single spheroids were seeded inside the matrix prior to gelation, after which TS complete media was added over the gelled matrix to prevent drying. Each spheroid was observed under microscopy, and cancer cell migration within the gel matrix was quantified by measuring the relative change in the occupied cell area, calculated as (Area at 72 h−Area at 0 h)/Area at 0 h [28].

ATP assay

GBM TSs were plated in 96-well plates at a density of 10^4 cells per well. After treatment, ATP levels were asessed using the CellTiter-Glo Luminescent Cell Viability Assay (Promega, Fitchburg, WI, USA) according to manufacturer protocols. Briefly, a volume of CellTiter-Glo Reagent equal to the volume of medium was added to each well, and luminescence was measured using a Centro LB 960 microplate luminometer (Berthold technologies, Oak Ride, TN, USA) after which cells were incubated at 24 °C for 10 min [29].

RNA preparation

Total RNA was isolated from the samples with TRIzol (Thermo Fisher Scientific, Waltham, MA, USA), according to the manufacturer's instructions [30]. A NanoDrop spectrophotometer (ThermoFisher Scientific) was used for confirmation of RNA quantity and purity.

RNA sequencing (RNA-seq) transcriptome analysis

RNA-seq transcriptome analysis of sham and low-frequency groups was conducted by Macrogen Inc., (Seoul, Korea) using the HiSequation

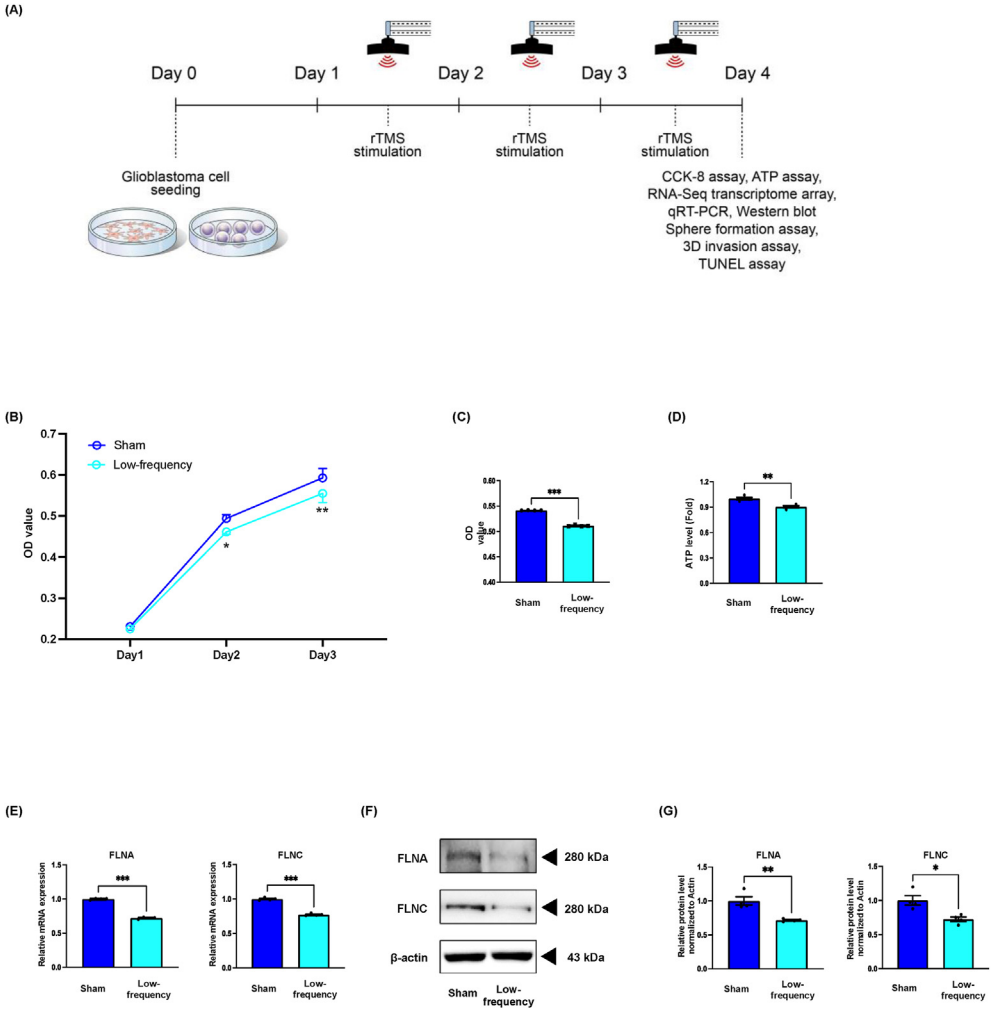

Fig. 1. Low-frequency rTMS suppresses cell proliferation by downregulating the expression of FLNA and FLNC in the *in vitro* GBM model. U87MG were used as the *in vitro* GBM model. The model was divided into two groups: a sham group (non-treated, $n = 4$) and a low-frequency group (treated with low-frequency rTMS, $n = 4$). (A) Schematic figure of low-frequency rTMS treatment on an *in vitro* GBM model. (B) Cell counting kit-8 (CCK-8) assay of the *in vitro* GBM model with or without low-frequency rTMS treatment. (C) Quantification of CCK-8 assay. (D) ATP assay of *in vitro* GBM model with or without low-frequency rTMS treatment. (E) The relative gene expression of FLNA and FLNC in the *in vitro* GBM model with or without low-frequency rTMS treatment, as detected by RT-qPCR. (F) Western blot analysis of FLNA and FLNC in the *in vitro* glioblastoma model with or without low-frequency rTMS treatment. (G) Quantification of Western blot signals for FLNA and FLNC. Values are presented as means ± standard error of the mean (SEM). Statistically significant differences are shown as $^*P < 0.05$, $^{**}P < 0.01$, $^{***}P < 0.001$.

2000 platform (Illumina, San Diego, CA, USA) for comparative analysis, as described previously [31].

Quantitative real-time reverse transcription-polymerase chain reaction

Quantitative real-time reverse transcription-polymerase chain reaction (RT-qPCR) was performed to validate the results of transcriptome analysis. According to the manufacturer's instructions, ReverTra Ace® qPCR RT Master Mix with gDNA Remover (Toyobo, Osaka, Japan) was used to prepare cDNA from total RNA. RT-qPCR to measure the mRNA levels of genes of interest was performed using qPCRBIO SyGreen Mix Hi-ROX (PCR BIOSYSTEMS, London, UK) in a StepOnePlus Real-Time PCR System (Applied Biosystems, Foster City, CA, USA). The $2^{-\Delta\Delta}$CT method was used to conduct data analysis [32]. Supplementary Table 1 lists the primers used for RT-qPCR.

Western blot

Total proteins were extracted from *in vitro* and *in vivo* experiments using RIPA buffer (Thermo Fisher Scientific, Waltham, MA, USA), and loaded onto SDS-PAGE gels (Bio-Rad, Hercules, CA, USA). Separated proteins were blotted onto polyvinylidene difluoride membranes (Invitrogen) with 20 % (v/v) methanol in transfer buffer (Invitrogen) at 15 V for 4 h at 4 °C. Membanes were blocked for 1 h using tris-buffered saline with 0.01 % Tween 20 (TBST) with 5 % skim milk (Difco, BD Biosciences, Oxford, UK. Blots were then washed three times with TBST for 10 min, then incubated overnight at 4 °C with primary antibodies specific for the following target proteins: p-PI3K (1:1000; Cell Signaling Technology, Cambridge, England), *p*-EphA2 (1:1000; Abcam, Cambridge, England), ERK, *p*-ERK, JNK, *p*-JNK, p38, p-p38, AKT, *p*-AKT, PI3K, mTOR, *p*-mTOR, Bax, Bcl-2, FLNA, *p*-EGFR, EGFR, EphA2, MMP2, MMP9, and β-actin (1:1000; Santa Cruz Biotechnology, Santa Cruz, CA, USA). After incubation, blots were washed three times with TBST and further incubated with horse-radish peroxidase–conjugated secondary antibody (1:3000; Santa Cruz) for 1hr at 24 °C. Blots were visualized with an enhanced chemiluminescence detection system (Amersham Pharmacia Biotech, Little Chalfont, UK).

Mouse orthotopic xenograft model

To establish an *in vivo* GBM model, male athymic nude mice (6–8 weeks old; Central Lab. Animal Inc., Seoul, Korea) were used. 5×10^5 U87MG TS cells suspended in 3 μl PBS were implanted into the right frontal lobe by stereotaxic injection using a Hamilton syringe (Donwoo Science Co., Seoul, Korea). After 1 week, mice were anesthetized with 1–2 % isoflurane and MRI experiments were performed with a 9.4-T Bruker BioSpec scanner (Ettlingen, Germany) running Paravision 5.1, using a 40-mm transreceiver coil. Following MRI analysis, mice with successful tumor xenografts were selected and subjected to the following experiments. MRI was taken once a week for 4 weeks. Mice in both sham and GBM groups were placed in a modified restrainer, which had an open space for direct exposure of the brain to the coil of the rTMS [33]. The distance between the center of the coil and the brain was approximately 1.0 cm to replicate the conditions used for previous *in vitro* experiments [34]. Mice were treated daily with 0.5 Hz rTMS for 10 min for the duration of the experiment. Mice in the TMZ control group were treated daily with 30 mg/kg temozolomide (Sigma Aldrich). While the sham group mice functioned as a positive control, the TMZ group mice functioned as the negative control. Approximately 21 d after the first treatment, some mice were euthanized, and the brains were carefully removed. Survival of the mice was analyzed using the Kaplan–Meier method.

Immunohistochemistry (IHC)

Brains removed from mice were fixed in 4 % paraformaldehyde. The brains were paraffin-embedded, and sections at a thickness of 5-μm were cut with a microtome and transferred onto adhesive slides as described previously [27]. Dako REAL EnVision Detection System (cat. no. K5007; DAKO) was used for 3,3′-diaminobenzidine tetrahydrochloride (DAB) staining and counterstaining was performed with hematoxylin (cat. no. GHS-3; Sigma). The sections were stained with antibody against FLNA, FLNC *p*-EphA, *p*-EGFR, *p*-ERK, *p*-JNK, p-p38, AKT, *p*-AKT, p-PI3K, *p*-mTOR, MMP2 and MMP9 (1:50). After staining, sections were analyzed using a confocal microscope (LSM700; Zeiss, Gottingen, Germany).

Terminal dUTP nick end-labeling (TUNEL) assay

For analysis of apoptosis, *in vitro* models were seeded on a cell culture slide (SPL Life Sciences, Gyeonggi-do, Korea). Sample slides from both *in vitro* and *in vivo* GBM models were fixed in 4 % paraformaldehyde. Afterward, the DeadEnd™ Fluorometric TUNEL system was utilized according to manufacturer protocols. DAPI was added to the samples before mounting with glass cover slides and fluorescent mounting medium. The LSM700 confocal microscope was used for imaging, as described above. The number of positively stained cells/total number of cells per specimen field was measured, and the percentage of positive cells was calculated. Four individual specimens per group were analyzed.

Bioluminescence imaging

Both *In vivo* imaging system (IVIS) and Living Image v4.2 software from Caliper Life Sciences were utilized to analyze bioluminescence. Mice were intraperitoneally injected with 100 μL of D-luciferin (30 mg/mL; Promega) and were placed under 2.5 % isoflurane anesthesia for 15 min before signal acquisition.

Ethics statement

The Association for Assessment and Accreditation of Laboratory Animal Care (AAALAC) and the Institutional Animal Care and Use Committee (IACUC) of Yonsei University Health System (permit number: 2022-0152) reviewed and approved the experiments of the study.

Statistical analysis

All data are expressed as means ± standard errors of the mean (SEM), and all experiments were repeated at least four times with four technical replicates in each group. The Statistical Package for Social Sciences v.25.0 (IBM Corp. Released 2015. IBM SPSS Statistics for Windows, v.25.0. Armonk, NY, USA) was used to conduct all statistical analyses. The significance of intergroup differences was estimated using Student's paired *t*-test, one-way analysis of variance (ANOVA), and Kaplan-Meier analysis as appropriate. Statistical significance was set at $P < 0.05$.

Results

Low-frequency rTMS suppresses cell proliferation by downregulating the expression of FLNA and FLNC in the in vitro GBM model

To establish an optimal low-frequency rTMS protocol for tumor suppressive effect on GBM, cell viability of U87MG cells was assessed after various frequencies of rTMS treatment. Although other frequency groups ranging from 0.1 to 1 Hz demonstrated reduced cell viability, the 0.5 Hz group exhibited the lowest cell viability. These findings suggest that the 0.5 Hz frequency is the most effective rTMS setting for GBM treatment (Supplementary Fig. 1 and Supplementary Table 2). Next, cell proliferation and ATP level were assessed using the CCK-8 assay and ATP assay to evaluate the effect of low-frequency rTMS on the *in vitro* GBM model (U87MG cells). In the CCK-8 assay, the proliferation of U87MG cells was significantly decreased after low-frequency treatment (Fig. 1B and C). ATP assay revealed notable decreases in ATP levels among U87MG cells after the treatment (Fig. 1D). Afterward, RNA-seq

transcriptome analysis was performed to identify differentially expressed genes in sham group and low-frequency group of U87MG cells. The expression of 11 transcripts and 6 transcripts was 1.5-fold higher and 1.5-fold lower, respectively, in the low-frequency group than in the sham group (Supplementary Table 3). Among downregulated genes in low-frequency group, our group focused on the differential expression of FLNA and FLNC, which are highly related to cancer development and the metastasis of GBM [35,36]. To validate the effect of low-frequency rTMS on the expression of FLNA and FLNC in U87MG cells, RT-qPCR and Western blot were conducted. The expression of genes and proteins of FLNA and FLNC was downregulated in low-frequency group compared to that in sham group (Fig. 1E–G).

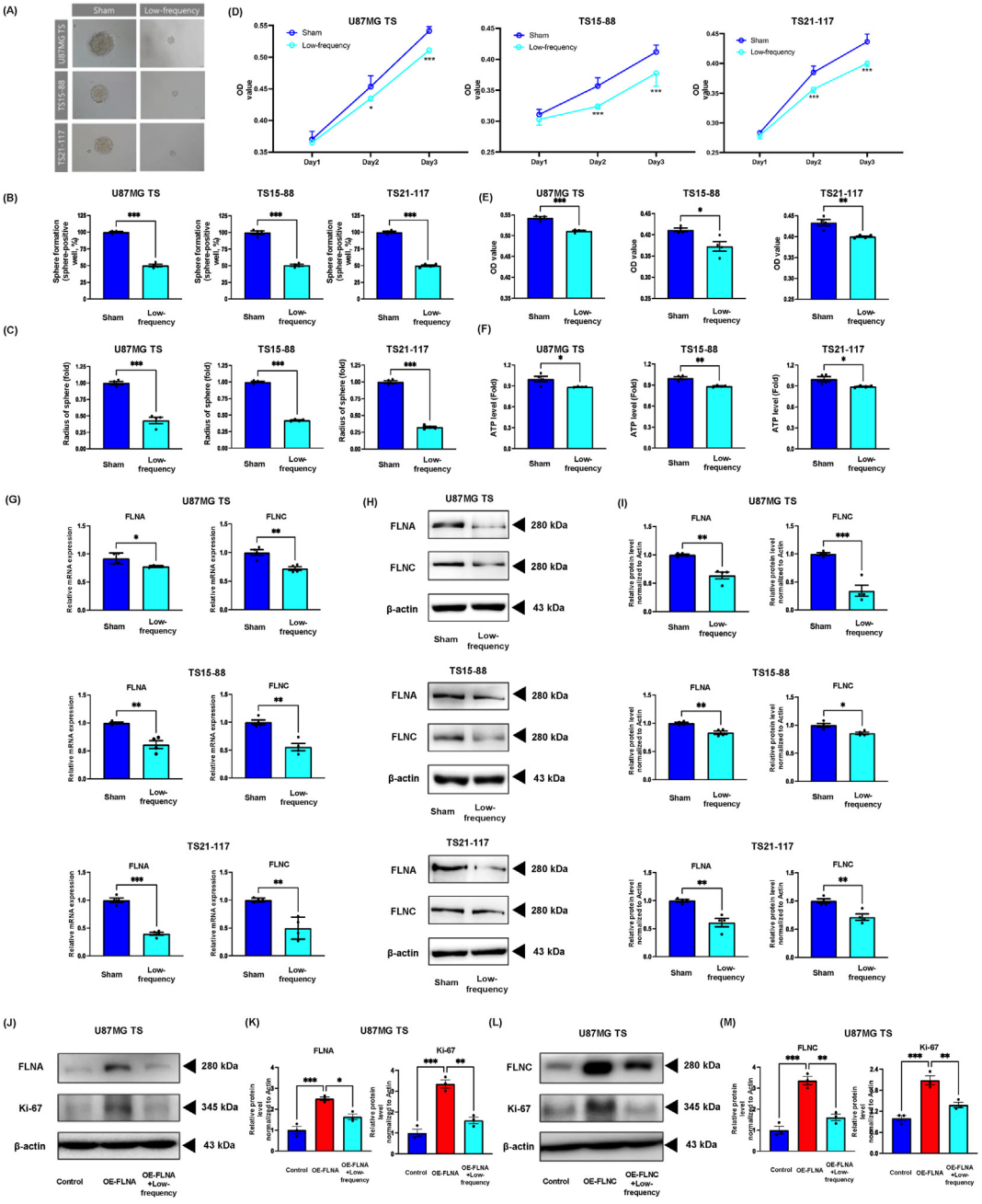

Fig. 2. Low-frequency rTMS suppresses cell proliferation and sphereformation by downregulating FLNA and FLNC expression in *in vitro* GBM models. U87MG TS, TS15-88, and TS21-117 were used as the *in vitro* GBM models. Models were divided into two groups: a sham group (non-treated, $n = 4$) and a low-frequency group (treated with low-frequency rMS, $n = 4$). (A) *In vitro* GBM sphere models with or without low-frequency rTMS treatment. (B) The ratio of sphere formation *in vitro* with or without low-frequency rTMS treatment. (C) The sphere radius of *in vitro* GBM models with or without low-frequency rTMS treatment. (D) Cell counting kit-8 (CCK-8) assay of the *in vitro* GBM models with or without low-frequency rTMS treatment. (E) Quantification of CCK-8 assay. (F) ATP assay of *in vitro* GBM models with or without low-frequency rTMS treatment. (G) The relative gene expression of FLNA and FLNC in the *in vitro* GBM models with or without low-frequency rTMS treatment, as detected by RT-qPCR. (H) Western blot analysis of FLNA and FLNC in the *in vitro* GBM models with or without low-frequency rTMS treatment. (I) Quantification of Western blot signals for FLNA and FLNC. (J) Western blot analysis of FLNA and Ki-67 in the in U87MG TS transfected with FLNA or pCNV6 and with or without low-frequency rTMS treatment (K) Quantification of Western blot signals for FLNA and Ki-67. (L) Western blot analysis of FLNC and Ki-67 in U87MG TS transduced with FLNC or pCNV6 and with or without low-frequency rTMS treatment (M) Quantification of Western blot signals for FLNC and Ki-67. Values are presented as means ± standard error of the mean (SEM). Statistically significant differences are shown as $^{*}P < 0.05$, $^{**}P < 0.01$, $^{***}P < 0.001$.

Low-frequency rTMS suppresses cell proliferation and sphere formation in the in vitro GBM model

To validate the effect of low-frequency rTMS on GBM, U87MG TS and primary GBM cells, which maintain more pronounced characteristics of genuine tumors under the TS culture condition, were used under the same experimental condition. The *in vitro* GBM models (U87MG TS, TS15-88, and TS21-117) were divided into sham and low-frequency groups (Fig. 2A). Low-frequency groups were treated with low-frequency rTMS and then assayed for sphere formation rate and size. The rates of sphere formation and sphere radii were significantly reduced after treatment (Fig. 2B and C). Additionally, consequent results from the CCK-8 assay indicated that the cell proliferation rates of the *in vitro* GBM models were significantly reduced after low-frequency treatment (Fig. 2D and E). ATP assays revealed marked decreases in ATP levels in the *in vitro* GBM models after the treatment (Fig. 2F). In addition, the gene expression and protein levels of FLNA and FLNC were downregulated in the low-frequency group compared to that in the sham group (Fig. 2G–I). To further determine whether low-frequency rTMS exerted its function via FLNA and FLNC, rescue experiments were performed. U87MG cells were first transfected with plasmids overexpressing either FLNA or FLNC under standard 2D cell culture conditions. Following transfection, the cells were cultured under tumor sphere conditions to induce sphere formation. These tumor spheres were then subjected to low-frequency rTMS treatment.

The results showed that the overexpression of FLNA or FLNC upregulated the expression of Ki-67, which is a marker for cell proliferation. Moreover, overexpression of FLNA or FLNC could rescue the expression of Ki-67 even after low-frequency rTMS treatment on the U87MG TS cells (Fig. 2J-M). These results indicate that overexpression of FLNA or FLNC downregulated the tumor suppressive effect of low-frequency rTMS on the *in vitro* GBM model.

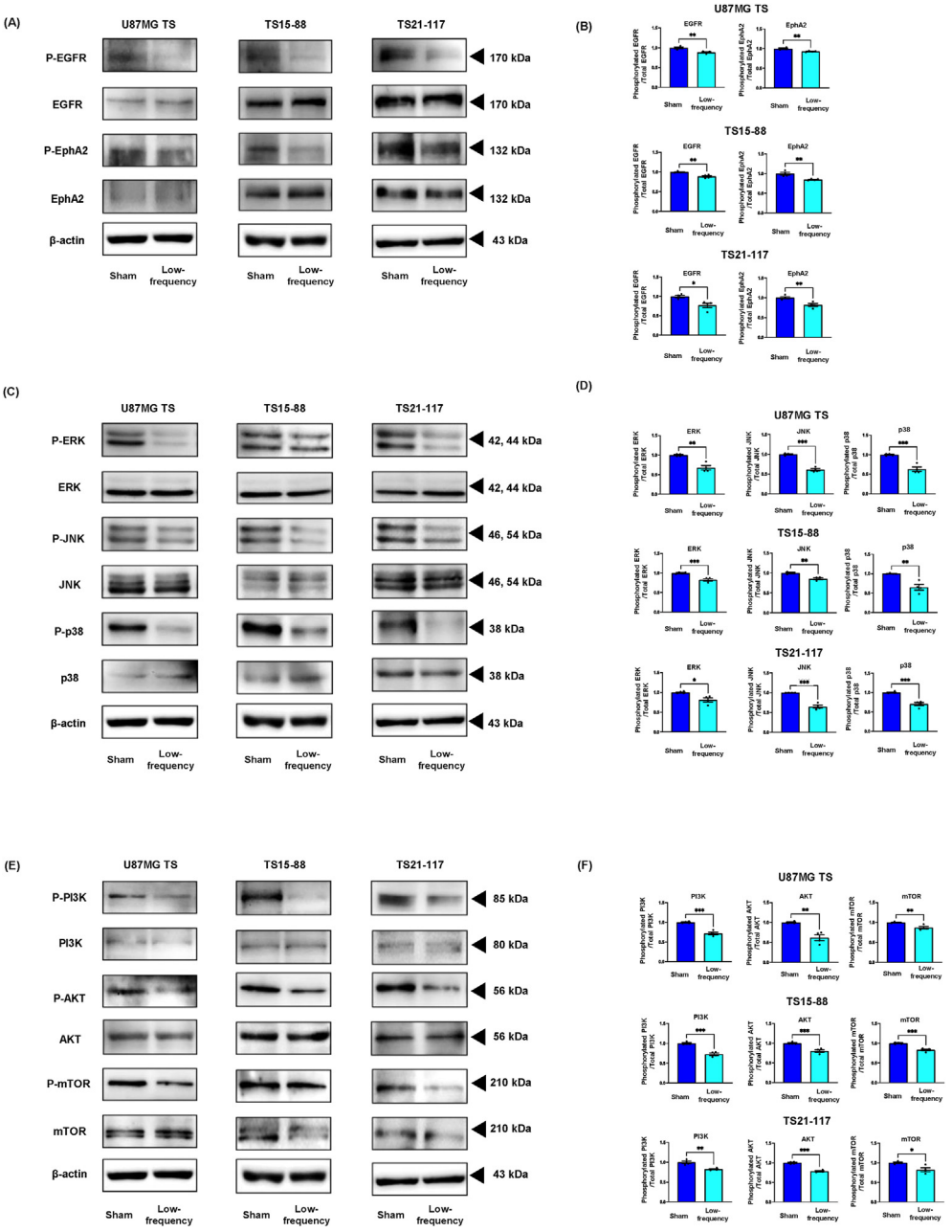

Fig. 3. Low-frequency rTMS downregulates the ERK/JNK/p38 and PI3K/AKT/mTOR pathway by suppressing EGFR and EphA2 activation in *in vitro* GBM models. (A) Western blot analysis of EGFR and EphA2 in the *in vitro* GBM models with or without low-frequency rTMS treatment. (B) Quantification of Western blot signals for EGFR and EphA2. (C) Western blot analysis of ERK, JNK, and p38 in the *in vitro* GBM models with or without low-frequency rTMS treatment. (D) Quantification of Western blot signals for ERK, JNK, and p38. (E) Western blot analysis of PI3K, AKT, and mTOR in the *in vitro* GBM models with or without low-frequency rTMS treatment. (F) Quantification of Western blot signals for PI3K, AKT, and mTOR. Values are presented as means ± standard error of the mean (SEM). Statistically significant differences are shown as $^{*}P < 0.05$, $^{**}P < 0.01$, $^{***}P < 0.001$.

Low-frequency rTMS inhibits ERK/JNK/p38 and PI3K/AKT/mTOR pathways via downregulation of EGF receptor and EphA2 activation through suppression of FLNA and FLNC in the in vitro GBM models

To further investigate the effects of low-frequency rTMS at a molecular level, the activation of EGFR, EphA2, and the ERK/JNK/p38 and PI3K/AKT/mTOR pathways was assessed by Western blot, since FLNA and FLNC were highly related to the activation of genes and pathways [35]. In U87MG TS, TS15-88, and TS21-117 cells, Western blot results showed that the levels of phosphorylated EGFR, EphA2, JNK, p38, ERK, PI3K, AKT, and mTOR were significantly decreased after low-frequency rTMS, indicating that the activation of EGFR and EphA2 (Fig. 3A and B), ERK/JNK/p38 (Fig. 3C and D), and PI3K/AKT/mTOR (Fig. 3E and F) signaling pathways were significantly inactivated.

Low-frequency rTMS induces apoptosis by downregulating ERK/JNK/p38 and PI3K/AKT/mTOR pathways in the in vitro GBM models

It is well known that the ERK/JNK/p38 and PI3K/AKT/mTOR pathways are major signaling pathways involved in cellular apoptosis [37]. To determine the effect of low-frequency rTMS on apoptosis in the *in vitro* GBM models, the expression of Bax and Bcl-2 were measured by RT-qPCR and Western blot, and the TUNEL assay was also performed. The expression of Bcl2, an anti-apoptotic marker, was significantly downregulated after low-frequency rTMS, whereas the expression of Bax, a pro-apoptotic marker, were upregulated in the *in vitro* GBM models (Fig. 4A–C). Moreover, TUNEL positive cells were notably increased in low-frequency group compared to that in sham group (Fig. 4D and E).

Low-frequency rTMS suppresses invasion of glioblastoma by downregulating the expression of MMP2 and MMP9 in the in vitro GBM models

In previous studies, overexpression of FLNC was related to enhanced GBM invasiveness by upregulating matrix metalloproteases (MMPs) [36, 38]. To investigate the effect of low-frequency rTMS on the invasion of GBM via downregulation of FLNC expression, the 3D invasion assay and analysis of the expression of MMP2 and MMP9 were employed. Results indicated that low-frequency rTMS had a suppressive effect on the invasion morphology of *in vitro* GBM models (Fig. 5A and B). Compared with the invaded area of the sham group, the invaded area of the low-frequency group was significantly smaller. Moreover, the gene and protein expression of both MMP2 and MMP9 was downregulated in the *in vitro* GBM models (Fig. 5C–E).

Low-frequency rTMS suppresses GBM progression by downregulating the expression of FLNA and FLNC in an in vivo GBM model

To investigate the effects of low-frequency rTMS on an *in vivo* GBM model, U87MG TS cells were injected into the right frontal cortex of nude mice (Fig. 6A). Tumor progression was monitored and measured using

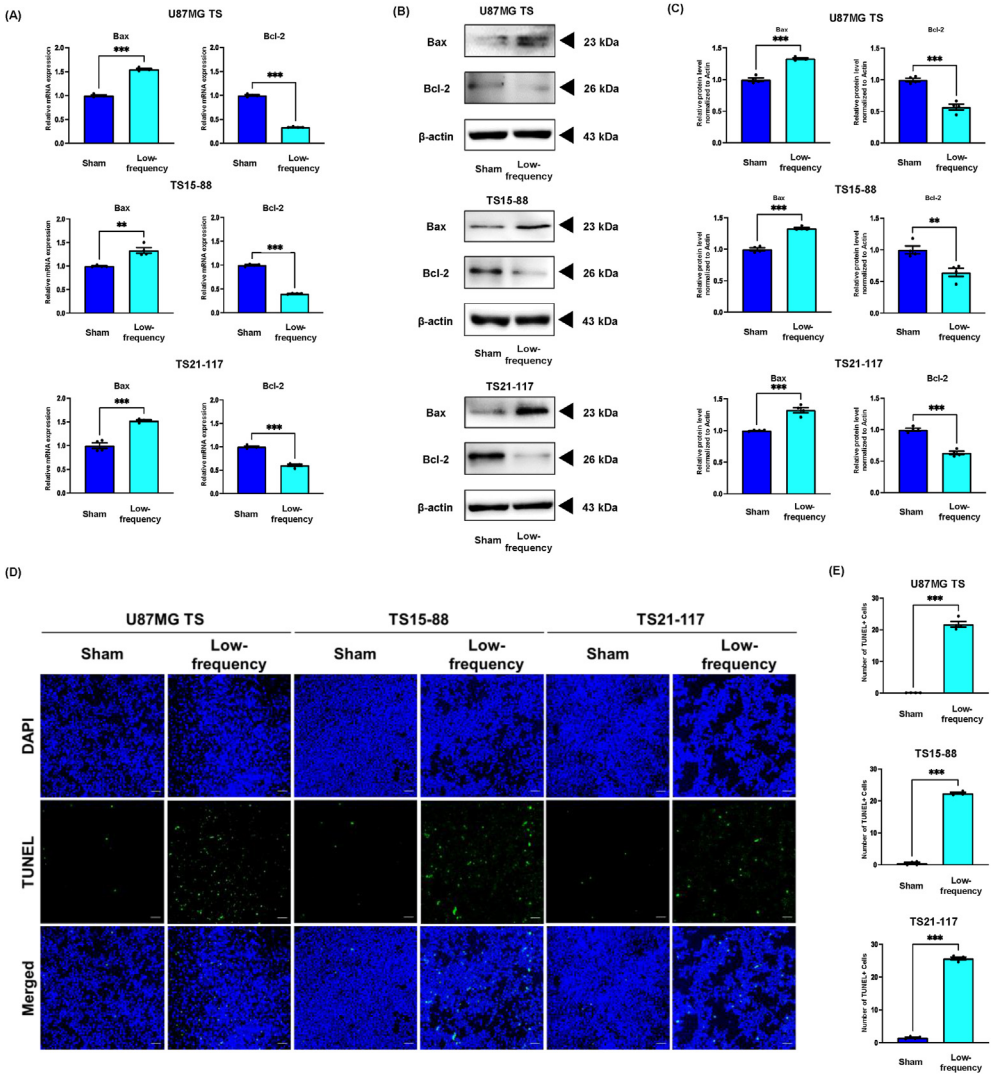

Fig. 4. Low-frequency rTMS induces apoptosis in the *in vitro* GBM models. (A) The relative gene expression of Bax and Bcl-2 detected by RT-qPCR. (B) Western blot analysis of Bax and Bcl-2 in the *in vitro* GBM models with or without low-frequency rTMS treatment. (C) Quantification of Western blot signals of Bax and Bcl-2. (D) TUNEL assay in the *in vitro* glioblastoma models with or without low-frequency rTMS treatment. (E) Quantification of TUNEL assay. Values are presented as means ± SEM. Scale bars = 100 μm. Statistically significant differences are shown as $^{**}P < 0.01$, $^{***}P < 0.001$.

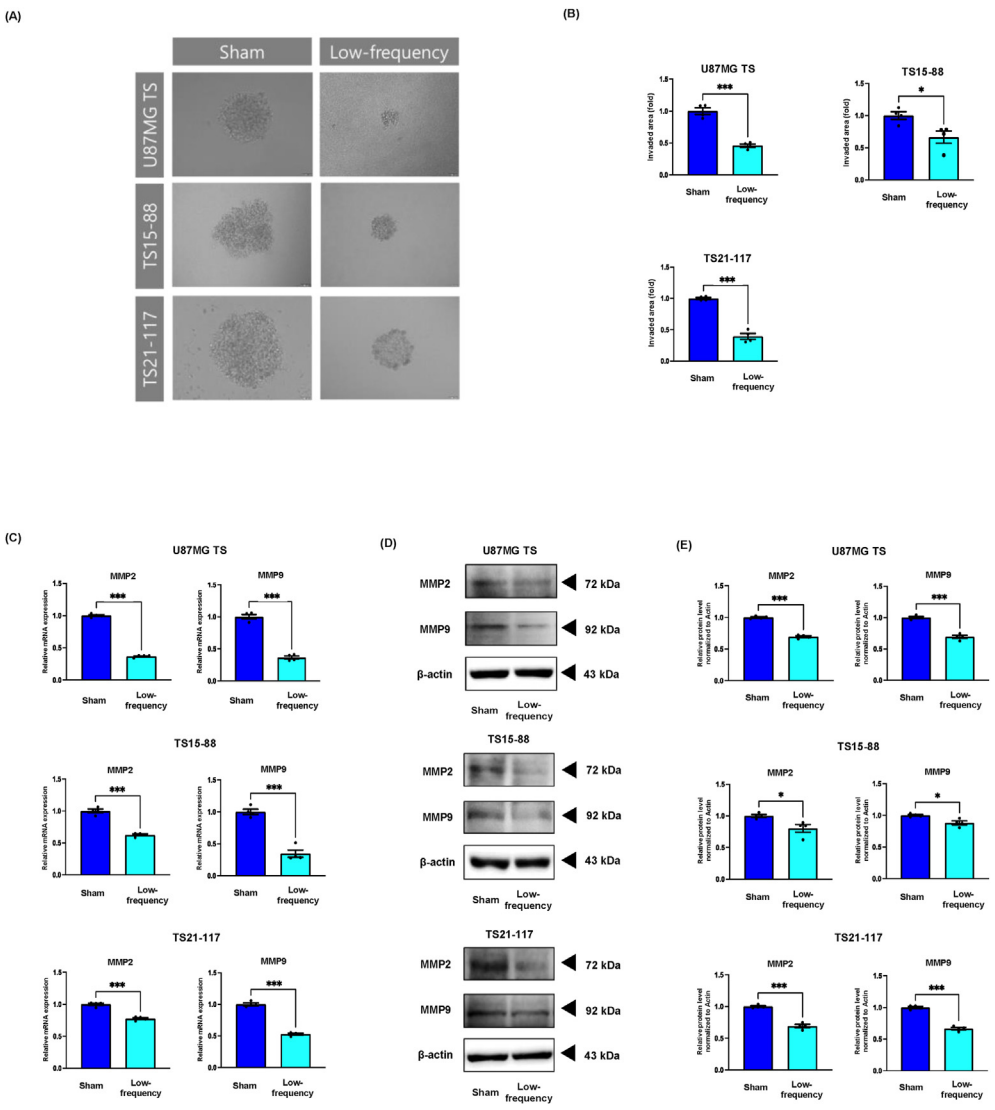

Fig. 5. Low-frequency rTMS suppresses invasion by downregulating the expression of MMP2 and MMP9 in the *in vitro* GBM models. (A) 3D invasion assay representing the invasive morphology of *in vitro* GBM models treated with or without low-frequency. (B) Quantification of 3D invasion assay. (C) The relative gene expression of MMP2 and MMP9 detected by RT-qPCR. (D) Western blot analysis of MMP2 and MMP9 in the *in vitro* GBM models with or without low-frequency rTMS treatment. (E) Quantification of Western blot signals for MMP2 and MMP9. Values are presented as means ± standard error of the mean (SEM). Statistically significant differences are shown as $*P < 0.05$, $***P < 0.001$.

MRI and bioluminescence imaging. The findings revealed that tumor sizes in the *in vivo* GBM model increased rapidly in the sham group, while it decreased in the low-frequency and TMZ groups. (Fig. 6B–G). Kaplan-Meier survival analysis showed that low-frequency and TMZ groups had significantly prolonged life span compared to sham group (Fig. 6H). Moreover, sectioned brain tissues with tumor mass were stained with FLNA, FLNC, Ki-67 antibodies, and H&E. Results showed fewer cells stained with FLNA, FLNC, and Ki-67 antibodies in the tumors of the low-frequency group and the TMZ group compared to that in the sham group (Fig. 6I and J). To determine the role of low-frequency rTMS on apoptosis in the *in vivo* GBM model, the TUNEL assay was conducted. TUNEL positive cells were increased in low-frequency group and TMZ group compared to that in the sham group (Fig. 6K-L). In addition, there were fewer cells stained with phosphorylated EphA, phosphorylated EGFR, phosphorylated ERK, phosphorylated JNK, phosphorylated p38, AKT, phosphorylated AKT, phosphorylated PI3K, phosphorylated mTOR, MMP2, and MMP9 antibodies in the tumors of the low-frequency group and TMZ group compared to that in the sham group. These results indicated that low-frequency rTMS inhibited ERK/JNK/p38 and PI3K/AKT/mTOR pathways via downregulating EGF receptor and EphA2 activation through suppression of FLNA and FLNC in the *in vivo* GBM model (Fig. 6M − N).

Discussion

rTMS is a non-invasive modality that stimulates the brain directly and is considered a potential therapeutic option for a variety of neurological diseases [39,40]. However, there have been different approaches to the use of rTMS as a treatment for cancer therapy. In previous studies, it has been suggested that low-frequency rMS treatment may have a potential benefit on neuroblastoma treatment [23,26]. Therefore, we explored the potential of low-frequency rTMS as one possible GBM treatment in this study.

Our results showed that cell proliferation, ATP levels and sphere formation of *in vitro* GBM models were significantly inhibited by low-frequency rTMS, indicating that low-frequency rTMS may potentially inhibit cell proliferation of GBM. RNA-seq transcriptome analysis between sham and low-frequency groups of *in vitro* GBM models showed that the expression of FLNA and FLNC was significantly suppressed after low-frequency rTMS. The results of RT-qPCR and Western blot confirmed the results of RNA-seq transcriptome analysis. In the rescue experiments, the overexpression of FLNA or FLNC decreased the effect of low-frequency rTMS on cell proliferation of *in vitro* GBM models. These results indicated that low-frequency rTMS may target FLNA and FLNC genes, which are closely associated with GBM proliferation, suggesting

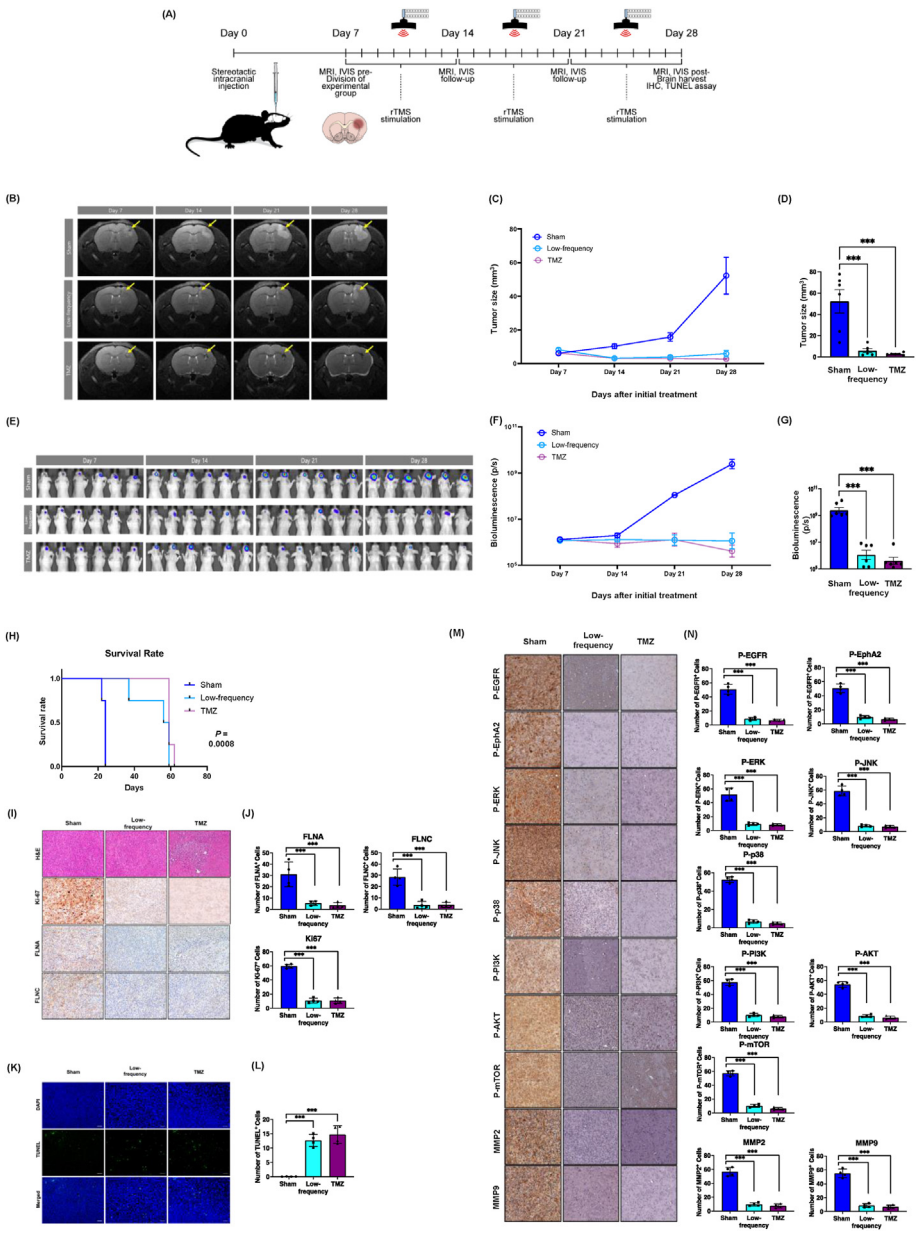

Fig. 6. Low-frequency rTMS suppressed tumor progression in an *in vivo* GBM model. The *in vivo* GBM model was divided into three groups: a sham group (non-treated), a low-frequency group (treated with low-frequency rTMS), and a TMZ group (treated with 30 mg/kg temozolomide). (A) Schematic figure of *in vivo* GBM model study. (B) MRI of brain tumor volume in sham, low-frequency, and TMZ groups ($n = 6$). (C) Tumor progression of the *in vitro* GBM model with or without low-frequency rTMS treatment or TMZ, as measured by tumor volume in the brain from MRI. (D) Final tumor size of the *in vitro* GBM model with or without low-frequency rTMS treatment, or TMZ. (E) Bioluminescence images of tumor volume on the brain of sham, low-frequency, and TMZ groups ($n = 6$). (F) Tumor progression of the *in vitro* GBM model with or without low-frequency rTMS treatment or TMZ, as measured by signal intensity of tumor mass in the brain. (G) Final signal intensity of tumor size in the *in vitro* GBM model with or without low-frequency rTMS treatment, or TMZ. (H) Survival rate for each group ($n = 4$) was estimated based on Kaplan-Meier curves. Log-rank test ($P = 0.008$). (I) Tumor mass stained by FLNA, FLNC and Ki67 antibody and H&E staining. (J) Quantification of cells stained with FLNA, FLNC and Ki67 antibody and H&E staining. (K) TUNEL assay in the *in vivo* GBM model with or without low-frequency rTMS treatment, or TMZ. (L) TUNEL assay quantification. (M) Tumor mass as stained by *p*-EphA, *p*-EGFR, *p*-ERK, *p*-JNK, p-p38, AKT, *p*-AKT, p-PI3K, *p*-mTOR, MMP2, and MMP9 antibody and H&E staining. (N) Quantification of cells stained with *p*-EphA, *p*-EGFR, *p*-ERK, *p*-JNK, p-p38, AKT, *p*-AKT, p-PI3K, *p*-mTOR, MMP2, and MMP9 staining. Values are presented as means ± SEM. Scale bars = 100 μm. Statistically significant differences are shown as $^{**}P < 0.01$, $^{***}P < 0.001$.

that these genes could be potential targets for GBM treatment [35,36]. For further exploration, the activation of EGFR and EphA2 was investigated, since the expression of FLNA and FLNC associates with EphA2 and EGFR during cancer cell proliferation and GBM migration [36,41]. In addition, the ERK/JNK/p38 and PI3K/AKT/mTOR pathways, which are linked to the activation of EGFR and EphA2 and are highly related to regulation of cancer proliferation, were investigated [42]. The results demonstrated that low-frequency rTMS downregulates ERK/JNK/p38 and PI3K/AKT/mTOR pathways by inhibiting the activation of EGFR and EphA2 in the *in vitro* GBM models. Through the downregulation of ERK/JNK/p38 and PI3K/AKT/mTOR pathways, cellular apoptosis was induced by low-frequency rTMS [43,44]. Low-frequency rTMS modulated the expression of Bax and Bcl-2 and increased TUNEL positive cells in the models. Altogether, these results indicated that low-frequency rTMS inhibited cell proliferation and induced apoptosis in the *in vitro* GBM models by downregulating the expression of FLNA and FLNC.

Moreover, FLNC is overexpressed in GBM patients and promotes GBM metastasis by regulating MMPs [36]. The activation of MMPs degrades the process of various extracellular matrix components and stimulates GBM invasion and metastasis [45]. MMP2 and MMP9 are highly overexpressed in GBM and contribute to remodeling the cellular cytoskeleton in the invasion and migration of glioblastoma [46]. The results indicated that GBM invasion, along with the expression of MMP2 and MMP9 genes and their corresponding gene products, was downregulated in *in vitro* GBM models following 3 days of low-frequency rTMS treatment. These findings suggest a direct correlation between GBM invasion and FLNC expression.

Furthermore, the effect of low-frequency rTMS on the *in vivo* GBM model was assessed by MRI and bioluminescence imaging. The mice bearing GBM reached the end point of their life span at 21 d while low-frequency rTMS and TMZ treatment groups showed significant tumor-suppressive effects, with prolongation of survival in the model. In addition, the expression of FLNA, FLNC and Ki-67 in the tumor mass was decreased and TUNEL positive cells were increased in low-frequency and TMZ groups compared to that in the sham group. These results indicated that low-frequency rTMS suppresses GBM progression and induces apoptosis by downregulating the expression of FLNA and FLNC in the *in vivo* GBM model.

In recent studies, various types of magnetic stimulation (MS) have been tested as potential non-invasive treatments for cancer therapy. It has been suggested that MS exerts effects on tumor angiogenesis by suppressing the volume of blood vessels in tumor [47]. Moreover, reports have demonstrated that MS induces apoptosis in cancers via the disruption of permeability of the mitochondrial membrane and an increase in ROS generation [48,49]. In addition, MS has been found to exhibit suppressive effects on cancer by inhibiting EGFR phosphorylation with the interference of asymmetric dimerization of the EGFR kinase domain [50]. Meanwhile research indicates that the effect of MS on cancer depends on several parameters, including the magnitude, frequency, and duration of the stimulation, since the sensitivity of cancers to MS varies depending on their cellular composition [51,52]. Previous studies have explored the effects of rMS by comparing various frequencies in reference to preclinical and clinical application protocols [3]. High-frequency rMS was found to cause an increase in cell proliferation, whereas low-frequency rMS elicited tumor suppressive effects on cell proliferation of neuroblastoma by inhibiting the Wnt/β-catenin signaling pathway [24–26]. Moreover, similar intensity of stimulation showed a suppressive effect on cell proliferation of glioma (18 mT) [22]. In the present study, low-frequency rTMS downregulated GBM progression via suppression of FLNA and FLNC. Therefore, it is possible to use low-frequency rTMS in conjunction with other therapies as a treatment strategy for cancer. However, further research should be conducted to elucidate the effect of low-frequency rTMS on epigenetic modification of cancer to more closely investigate the fundamental mechanism of action. In addition, it will be imperative to establish targeted rTMS methods to precisely locate the tumor mass for future clinical applications, in order to mitigate the adverse effects of low-frequency rTMS on healthy tissue.

In summary, the results of this study suggest that low-frequency rTMS may have a tumor suppressive effect on GBM progression. In addition, the underlying mechanism of low-frequency rTMS on GBM appears to be positively related to the downregulation of expression of FLNA and FLNC. These findings indicate that low-frequency rTMS has a potential benefit on GBM treatment. Therefore, the present study sheds light on the mechanism and effectivity of low-frequency rTMS as a potential treatment for non-invasive cancer therapy.

Author contributions

SJ and SHI: Lead, Investigation, Formal analysis, Funding acquisition, Writing – original draft, Writing – review & editing. **SHK:** Conceptualization, Funding acquisition, Supervision, **DB:** Investigation, Formal analysis, Writing – original draft, Writing – review & editing. **J-KS:** Investigation. **S-GK:** Conceptualization, Formal analysis, Supervision. **JHC**: Investigation. **GRN:** Investigation, Writing – original draft, Writing – review & editing. **D-WL:** Investigation. **AB and S-RC:** Conceptualization, Formal analysis, Funding acquisition, Supervision, Writing – original draft, Writing – review & editing.

Data availability

The datasets used and/or analyzed during the current study are available from the corresponding author upon reasonable request.

Ethics approval and consent to participate

The Association for Assessment and Accreditation of Laboratory Animal Care (AAALAC) and the Institutional Animal Care and Use Committee (IACUC) of Yonsei University Health System (permit number: 2022-0152) reviewed and approved the experiments of the study.

Consent for publication

Not applicable.

Funding

This work was supported by the National Research Foundation of Korea (NRF) grant funded by the Korea government (MSIT) (RS-2022-NR069331 and RS-2024-00354247), the Korean Fund for Regenerative Medicine (KFRM) grant funded by the Korea government (the Ministry of Science and ICT, the Ministry of Health & Welfare) (21A0202L1), the Korean Health Technology R&D Project through the Korea Health Industry Development Institute (KHIDI), funded by the Ministry of Health & Welfare, Republic of Korea (HI22C1588 and HI21C1314), and a grant from Hyundai Motor Chung Mong-Koo Foundation.

Declaration of competing interest

The authors declare that they have no known competing financial interests or personal relationships that could have appeared to influence the work reported in this paper.

Acknowledgments

The authors thank Medical Illustration & Design, part of the Medical Research Support Services of Yonsei University College of Medicine, for all artistic support related to this work. In addition, we would like to thank Editage (www.editage.co.kr) for English language editing.

Appendix A. Supplementary data

Supplementary data to this article can be found online at https://doi.org/10.1016/j.neurot.2025.e00569.

References

[1] Barker AT, Jalinous R, Freeston IL. Non-invasive magnetic stimulation of human motor cortex. Lancet 1985;1(8437):1106–7.
[2] Huang YZ, Edwards MJ, Rounis E, Bhatia KP, Rothwell JC. Theta burst stimulation of the human motor cortex. Neuron 2005;45(2):201–6.
[3] Wassermann EM, Lisanby SH. Therapeutic application of repetitive transcranial magnetic stimulation: a review. Clin Neurophysiol 2001;112(8):1367–77.
[4] Hoogendam JM, Ramakers GM, Di Lazzaro V. Physiology of repetitive transcranial magnetic stimulation of the human brain. Brain Stimul 2010;3(2):95–118.
[5] Fitzgerald PB, Brown TL, Daskalakis ZJ. The application of transcranial magnetic stimulation in psychiatry and neurosciences research. Acta Psychiatr Scand 2002;105(5):324–40.
[6] George MS, Nahas Z, Molloy M, Speer AM, Oliver NC, Li XB, et al. A controlled trial of daily left prefrontal cortex TMS for treating depression. Biol Psychiatry 2000;48(10):962–70.
[7] Kimbrell TA, Little JT, Dunn RT, Frye MA, Greenberg BD, Wassermann EM, et al. Frequency dependence of antidepressant response to left prefrontal repetitive transcranial magnetic stimulation (rTMS) as a function of baseline cerebral glucose metabolism. Biol Psychiatry 1999;46(12):1603–13.
[8] Pascual-Leone A, Valls-Sole J, Brasil-Neto JP, Cammarota A, Grafman J, Hallett M. Akinesia in Parkinson's disease. II. Effects of subthreshold repetitive transcranial motor cortex stimulation. Neurology 1994;44(5):892–8.
[9] Ziemann U, Paulus W, Rothenberger A. Decreased motor inhibition in Tourette's disorder: evidence from transcranial magnetic stimulation. Am J Psychiatr 1997;154(9):1277–84.
[10] Menkes DL, Gruenthal M. Slow-frequency repetitive transcranial magnetic stimulation in a patient with focal cortical dysplasia. Epilepsia 2000;41(2):240–2.
[11] Fan H, Song Y, Cen X, Yu P, Biro I, Gu Y. The effect of repetitive transcranial magnetic stimulation on lower-limb motor ability in stroke patients: a systematic review. Front Hum Neurosci 2021;15:620573.
[12] Choung JS, Kim JM, Ko MH, Cho DS, Kim M. Therapeutic efficacy of repetitive transcranial magnetic stimulation in an animal model of Alzheimer's disease. Sci Rep 2021;11(1):437.
[13] Shi C, Yu X, Cheung EF, Shum DH, Chan RC. Revisiting the therapeutic effect of rTMS on negative symptoms in schizophrenia: a meta-analysis. Psychiatry Res 2014;215(3):505–13.
[14] Tan AC, Ashley DM, Lopez GY, Malinzak M, Friedman HS, Khasraw M. Management of glioblastoma: state of the art and future directions. CA Cancer J Clin 2020;70(4):299–312.
[15] Taphoorn MJ, Sizoo EM, Bottomley A. Review on quality of life issues in patients with primary brain tumors. Oncologist 2010;15(6):618–26.
[16] Reardon DA, Wen PY. Therapeutic advances in the treatment of glioblastoma: rationale and potential role of targeted agents. Oncologist 2006;11(2):152–64.

[17] Van Meir EG, Hadjipanayis CG, Norden AD, Shu HK, Wen PY, Olson JJ. Exciting new advances in neuro-oncology: the avenue to a cure for malignant glioma. CA Cancer J Clin 2010;60(3):166–93.
[18] Raffa G, Quattropani MC, Germano A. When imaging meets neurophysiology: the value of navigated transcranial magnetic stimulation for preoperative neurophysiological mapping prior to brain tumor surgery. Neurosurg Focus 2019; 47(6).
[19] Einstein EH, Dadario NB, Khilji H, Silverstein JW, Sughrue ME, D'Amico RS. Transcranial magnetic stimulation for post-operative neurorehabilitation in neuro-oncology: a review of the literature and future directions. J Neuro Oncol 2022; 157(3):435–43.
[20] Yamaguchi S, Ogiue-Ikeda M, Sekino M, Ueno S. Effects of magnetic stimulation on tumors and immune functions. IEEE Trans Magn 2005;41(10):4182–4.
[21] Yamaguchi S, Ogiue-Ikeda M, Sekino M, Ueno S. Effects of pulsed magnetic stimulation on tumor development and immune functions in mice. Bioelectromagnetics 2006;27(1):64–72.
[22] Xu W, Sun J, Le Y, Chen J, Lu X, Yao X. Effect of pulsed millisecond current magnetic field on the proliferation of C6 rat glioma cells. Electromagn Biol Med 2019;38(3):185–97.
[23] Lee JY, Park HJ, Kim JH, Cho BP, Cho SR, Kim SH. Effects of low- and high-frequency repetitive magnetic stimulation on neuronal cell proliferation and growth factor expression: a preliminary report. Neurosci Lett 2015;604:167–72.
[24] Baek A, Kim JH, Pyo S, Jung JH, Park EJ, Kim SH, et al. The differential effects of repetitive magnetic stimulation in an in vitro neuronal model of ischemia/reperfusion injury. Front Neurol 2018;9:50.
[25] Baek A, Park EJ, Kim SY, Nam BG, Kim JH, Jun SW, et al. High-frequency repetitive magnetic stimulation enhances the expression of brain-derived neurotrophic factor through activation of Ca2+-calmodulin-dependent protein kinase II-cAMP-Response element-binding protein pathway. Front Neurol 2018:9.
[26] Jo S, Im SH, Seo D, Ryu H, Kim SH, Baek D, et al. Low-frequency repetitive magnetic stimulation suppresses neuroblastoma progression by downregulating the Wnt/beta-catenin signaling pathway. Bioelectrochemistry 2022;147:108205.
[27] Park J, Shim JK, Kang JH, Choi J, Chang JH, Kim SY, et al. Regulation of bioenergetics through dual inhibition of aldehyde dehydrogenase and mitochondrial complex I suppresses glioblastoma tumorspheres. Neuro Oncol 2018; 20(7):954–65.
[28] Kim EH, Lee JH, Oh Y, Koh I, Shim JK, Park J, et al. Inhibition of glioblastoma tumorspheres by combined treatment with 2-deoxyglucose and metformin. Neuro Oncol 2017;19(2):197–207.
[29] Jeong H, Park J, Shim JK, Lee JE, Kim NH, Kim HS, et al. Combined treatment with 2'-hydroxycinnamaldehyde and temozolomide suppresses glioblastoma tumorspheres by decreasing stemness and invasiveness. J Neuro Oncol 2019; 143(1):69–77.
[30] Chomczynski P. A reagent for the single-step simultaneous isolation of RNA, DNA and proteins from cell and tissue samples. Biotechniques 1993;15(3):532–4. 536-537.
[31] Baek A, Kim M, Kim SH, Cho SR, Kim HJ. Anti-inflammatory effect of DNA polymeric molecules in a cell model of osteoarthritis. Inflammation 2018;41(2):677–88.
[32] Fan M, Mi R, Yew DT, Chan WY. Analysis of gene expression following sciatic nerve crush and spinal cord hemisection in the mouse by microarray expression profiling. Cell Mol Neurobiol 2001;21(5):497–508.
[33] Lenz M, Galanis C, Muller-Dahlhaus F, Opitz A, Wierenga CJ, Szabo G, et al. Repetitive magnetic stimulation induces plasticity of inhibitory synapses. Nat Commun 2016;7:10020.
[34] Zhang C, Lu R, Wang L, Yun W, Zhou X. Restraint devices for repetitive transcranial magnetic stimulation in mice and rats. Brain Behav 2019;9(6):e01305.
[35] Chantaravisoot N, Wongkongkathep P, Loo JA, Mischel PS, Tamanoi F. Significance of filamin A in mTORC2 function in glioblastoma. Mol Cancer 2015;14:127.
[36] Kamil M, Shinsato Y, Higa N, Hirano T, Idogawa M, Takajo T, et al. High filamin-C expression predicts enhanced invasiveness and poor outcome in glioblastoma multiforme. Br J Cancer 2019;120(8):819–26.
[37] Zhang L, Wang HD, Xu JG, Zhu JH, Ding K. Inhibition of cathepsin S induces autophagy and apoptosis in human glioblastoma cell lines through ROS-mediated PI3K/AKT/mTOR/p70S6K and JNK signaling pathways. Toxicol Lett 2014;228(3): 248–59.
[38] Liu Y, Zheng J, Zhang Y, Wang Z, Yang Y, Bai M, et al. Fucoxanthin activates apoptosis via inhibition of PI3K/Akt/mTOR pathway and suppresses invasion and migration by restriction of p38-MMP-2/9 pathway in human glioblastoma cells. Neurochem Res 2016;41(10):2728–51.
[39] Kobayashi M, Pascual-Leone A. Transcranial magnetic stimulation in neurology. Lancet Neurol 2003;2(3):145–56.
[40] Klomjai W, Katz R, Lackmy-Vallee A. Basic principles of transcranial magnetic stimulation (TMS) and repetitive TMS (rTMS). Ann Phys Rehabil Med 2015;58(4): 208–13.
[41] Tamura Y, Nakamizo Y, Watanabe Y, Kimura I, Katoh H. Filamin A forms a complex with EphA2 and regulates EphA2 serine 897 phosphorylation and glioblastoma cell proliferation. Biochem Biophys Res Commun 2022;597:64–70.
[42] Kim HJ, Ryu KJ, Kim M, Kim T, Kim SH, Han H, et al. RhoGDI2-Mediated Rac1 recruitment to filamin A enhances Rac1 activity and promotes invasive abilities of gastric cancer cells. Cancers 2022;14(1).
[43] Wu YL, Maachani UB, Schweitzer M, Singh R, Wang M, Chang R, et al. Dual inhibition of PI3K/AKT and MEK/ERK pathways induces synergistic antitumor effects in diffuse intrinsic pontine glioma cells. Transl Oncol 2017;10(2):221–8.
[44] Wong KK, Engelman JA, Cantley LC. Targeting the PI3K signaling pathway in cancer. Curr Opin Genet Dev 2010;20(1):87–90.
[45] Ramachandran RK, Sorensen MD, Aaberg-Jessen C, Hermansen SK, Kristensen BW. Expression and prognostic impact of matrix metalloproteinase-2 (MMP-2) in astrocytomas. PLoS One 2017;12(2):e0172234.
[46] VanMeter TE, Rooprai HK, Kibble MM, Fillmore HL, Broaddus WC, Pilkington GJ. The role of matrix metalloproteinase genes in glioma invasion: co-dependent and interactive proteolysis. J Neuro Oncol 2001;53(2):213–35.
[47] Cameron IL, Markov MS, Hardman WE. Optimization of a therapeutic electromagnetic field (EMF) to retard breast cancer tumor growth and vascularity. Cancer Cell Int 2014;14(1):125.
[48] Gurhan H, Bruzon R, Kandala S, Greenebaum B, Barnes F. Effects induced by a weak static magnetic field of different intensities on HT-1080 fibrosarcoma cells. Bioelectromagnetics 2021;42(3):212–23.
[49] Sharpe MA, Baskin DS, Pichumani K, Ijare OB, Helekar SA. Rotating magnetic fields inhibit mitochondrial respiration, promote oxidative stress and produce loss of mitochondrial integrity in cancer cells. Front Oncol 2021;11:768758.
[50] Zhang L, Wang J, Wang H, Wang W, Li Z, Liu J, et al. Moderate and strong static magnetic fields directly affect EGFR kinase domain orientation to inhibit cancer cell proliferation. Oncotarget 2016;7(27):41527–39.
[51] Zhu Y, Wang S, Long H, Zhu J, Jian F, Ye N, et al. Effect of static magnetic field on pain level and expression of P2X3 receptors in the trigeminal ganglion in mice following experimental tooth movement. Bioelectromagnetics 2017;38(1):22–30.
[52] Sengupta S, Balla VK. A review on the use of magnetic fields and ultrasound for non-invasive cancer treatment. J Adv Res 2018;14:97–111.